J. Biochem. 2010;147(4):511–522 doi:10.1093/jb/mvp197

JB THE JOURNAL OF BIOCHEMISTRY

Cloning, expression and characterization of the catalase–peroxidase (KatG) gene from a fast-growing *Mycobacterium* sp. strain JC1 DSM 3803

Received October 6, 2009; accepted November 16, 2009; published online November 23, 2009

Hyun-Il Lee[1,*], Ji-Hyun Yoon[1], Ji-Sun Nam[1], Young-Min Kim[2] and Young-Tae Ro[1,†]

[1]Department of Biochemistry, Graduate School of Medicine, Konkuk University, Seoul 134-701, Korea and [2]Department of Biology, College of Life Science and Biotechnology, Yonsei University, Seoul 120-749, Korea

*Present address: Department of Orthopedic Surgery, Samsung Medical Center, Seoul 135-710, Korea.

†Young-Tae Ro, Laboratory of Biochemistry, Graduate School of Medicine, Konkuk University, Seoul 134-701, Korea, Tel: +82-2-2030-7825, Fax: +82-2-2049-6192, E-mail: ytaero@kku.ac.kr

The gene encoding a catalase–peroxidase (KatG) was cloned from chromosomal DNA of a fast-growing *Mycobacterium* sp. strain JC1 DSM 3803. The nucleotide sequence of a 5.7 kb *Eco*RI fragment containing the *katG* and its flanking regions was determined. The fragment (5,706 bps) contained two complete open reading frames (ORFs) encoding putative ferric uptake regulator A (FurA) and KatG proteins. The cloned gene, *katG*, had an ORF of 2241 nt, encoding a protein with calculated molecular mass of 81,748 Da. The *furA* was located in the upstream of the *katG* with the same transcriptional direction and there was a 38 bp gap space between them. The deduced KatG and FurA protein sequences showed significant homologies to KatG2 and Fur2 of *Mycobacterium smegmatis* and clustered with other mycobacterial KatG and Fur-like proteins in phylogenetic trees, respectively. The recombinant KatG overproduced in *Escherichia coli* was nearly indistinguishable from the native JC1 catalase–peroxidase in enzymatic properties and also possessed the resistance to organic solvents, indicating that the cloned *katG* truly encodes the *Mycobacterium* sp. JC1 catalase–peroxidase. Difference spectroscopy revealed Mn(II) binding near the haem of the KatG. Transcript analysis of the *furA–katG* using RT–PCR suggests that the *katG* is independently transcribed from the *furA*.

Keywords: catalase–peroxidise/*furA-katG* locus/ Mn(II) binding/recombinant protein expression/ transcription analysis.

Abbreviations: CP, catalase–peroxidase; DIG, digoxigenin; FurA, ferric uptake regulator A; INH, isoniazid; LB, Luria-Bertani; MnP, manganese peroxidase; ORF, open reading frame; PPS, polypurine sequence; SD sequence, Shine-Dalgarno sequence; SMB, standard mineral base.

Catalase–peroxidase (CP or KatG) is a haem protein that exhibits both catalase and peroxidase activities. Catalase decomposes H_2O_2 to O_2 and H_2O, whereas peroxidase reduces H_2O_2 to H_2O with an external reductant. In contrast to the ubiquitous catalases in bacteria, plant and animal, KatG is restricted to prokaryotes and some fungi (*1*, *2*). KatG has several unique features different from the typical mono-functional catalase, in that KatG is inhibited by cyanide and azide, but not by 3-amino-1,2,4-triazol, which is a traditional catalase inhibitor (*3*). Moreover, KatG is active only in a limited range of temperatures, whereas the typical catalase is relatively heat-resistant.

KatGs have been widely investigated in a variety of bacteria including mycobacteria such as *Mycobacterium tuberculosis* and *M. smegmatis* (*4–6*). They play a crucial role in defending against oxidative stress generated by aerobic oxygen metabolism or phagocytic attack from macrophages or neutrophils. Among those, mycobacterial KatG has raised special attention due to its participation in mycobacterial virulence. Since *M. tuberculosis* is an intracellular pathogen residing in macrophages, KatG is essential for survival from reactive oxygen intermediates produced by macrophages (*7*, *8*). Ironically, however, KatG is also important for activation of the front-line antituberculosis pro-drug, isoniazid (INH) (*9*); hence, *M. tuberculosis* containing genetic deletion of *katG* or mutation in *katG* acquired a resistance to INH (*10*, *11*).

Mycobacterium sp. strain JC1 DSM 3803 isolated from Korea soil has versatile metabolic activities including a unique ability to utilize carbon monoxide (CO), methanol and benzylamine as sole carbon and energy sources (*12–15*). This bacterium possesses three different catalases including a CP (*16*). Only the CP was highly expressed in either CO- or methanol-grown cells, suggesting that the enzyme may have important roles in CO/methanol metabolism and protection against the oxidative stress by the toxic compounds (*17*). Moreover, the CP expression was strongly stimulated by a NO-producing agent, sodium nitroprusside (*18*), suggesting its role in nitrosative defence. The purified protein from methanol-grown *Mycobacterium* sp. JC1 showed typical characteristics of bi-functional CP in kinetic assays, with the exception of resistance to organic solvents, which is a property of true catalase. The CP also revealed striking immunological similarities to other mycobacterial KatGs (*18*). Although the CP of *Mycobacterium* sp. JC1 shares several common properties with other mycobacterial KatGs, therefore we raise a question whether the CP gene has evolved differently from the respective catalase–peroxidase

gene (*katG*) family, since the protein possessed a property of typical catalase such as the resistance to organic solvents.

In order to address this question, we cloned a DNA fragment containing a *furA–katG* locus using a probe generated from two degenerated primers based on the conserved sequences from mycobacterial KatGs. Sequence homology and phylogenetic studies show that the *Mycobacterium* sp. JC1 CP gene is in one of the catalase–peroxidase gene families and it diverges from the mycobacterial *katG* family. Transcript analysis of the *furA–katG* using RT–PCR suggests that the *katG* is independently transcribed from the *furA*. The recombinant KatG actively overproduced in *E. coli* is nearly indistinguishable from the native JC1 CP in enzymatic properties, and it also retains the resistance to organic solvents (ethanol/chloroform), indicating that the cloned *katG* truly encodes the novel *Mycobacterium* sp. JC1 CP.

Materials and Methods

Bacterial strains, plasmids and cultivation

Mycobacterium sp. JC1 was cultivated at 37°C in standard mineral base (SMB) medium (*19*) supplemented with 0.5% (v/v) methanol. *Escherichia coli* strains for cloning and expressing KatG gene were grown at 37°C in Luria–Bertani (LB) medium. Growth was measured with a spectrophotometer by determination of turbidity at 436 nm.

DNA manipulation

Chromosomal DNA was isolated from *Mycobacterium* sp. JC1 grown in SMB-methanol medium according to a method previously reported (*20*). Plasmid and cosmid DNAs in *E. coli* were isolated by using QIAamp DNA mini kit as the manufacturer's instruction (Qiagen, USA).

Construction of a genomic cosmid library of Mycobacterium sp. JC1

Total genomic library of *Mycobacterium* sp. JC1 was constructed by using a pWEB cosmid cloning kit (Epicentre, USA) in accordance with the manufacturer's instruction. Briefly, chromosomal DNA was fragmented by passing it through a syringe needle and end-repaired to generate blunt ends. The 35–40-kb-sized DNA fragments were used for in-gel ligation into the pWEB cosmid vector. The ligated cosmids were packaged in lambda phage using MaxPlax packaging extracts, transfected into *E. coli* EPI100-T1^{R} cells and plated for colony formation. A total of 720 colonies, which are sufficient for covering the entire genome with 99% probability, were individually picked by toothpicks, transferred and grown in number-marked LB-ampicillin agar plates for cosmid library screening.

Random-primed probe synthesis

Two degenerated primers, JCP-F (5′-TCGCAGSMSTGGTGG CC-3′) and JCP-R (5′-ACGTAGATSAGSCCCAT-3′), were synthesized to amplify the region covering the *katG* of *Mycobacterium* sp. JC1, based on the consensus amino acid sequences SQ(P/D)WWP and MGLIYV, respectively, that are present at near the N-termini of KatGs (*21*). The PCR amplification was performed in a 50 µl reaction mixture containing 100 ng genomic DNA, 50 pmol of each primer and 1.5 unit of Han-Taq polymerase (Genenmed, Korea). The amplification condition was as follows: after primary denaturation for 3 min at 95°C, 30 cycles each of denaturation for 40 s at 95°C, annealing for 40 s at 52°C and elongation for 40 s at 72°C were performed, and then post-elongation was carried out for 10 min at 72°C. The PCR products were directly cloned into pCR2.1 cloning vector (Invitrogen, USA) as the manufacturer's instruction and the clones containing the PCR fragment were screened by 1% agarose gel electrophoresis after *Eco*RI digestion. A positive clone (pCR-JCP1) was selected and subjected to automated DNA sequencing protocol (Takara Korea, Korea), and then the DNA sequence was analysed by using ExPASy proteomics server (http://ca.expasy.org/) for finding the KatG sequence homology.

For probe preparation, the *Eco*RI-digested PCR fragment of pCR-JCP1 was eluted from an agarose gel after electrophoresis and purified with the QIAquick gel extraction kit (Qiagen, USA). The gel-purified fragment was labeled with a digoxigenin (DIG)-high prime DNA labelling kit according to the instructions of the manufacturer (Roche, Germany) and the random-primed probe (JCP probe) was used for colony lift hybridization and Southern blotting procedures.

Southern hybridization and katG gene cloning

From colony lift hybridization, a cosmid DNA (pWEBJCP6-72) revealing positive result to the JCP probe was digested with several restriction enzymes, subjected to electrophoresis, and then transferred to Hybond-N^{+} membrane (Amersham, USA) by capillary blotting. The prehybridization and hybridization time were 1 and 16 h at 42°C, respectively, and all the steps were carried out according to the DIG application manual (Roche, USA). From Southern analysis, an ~6-kb sized *Eco*RI DNA fragment showing strong signal to the JCP probe was eluted from an agarose gel, purified and cloned into pBluescript II KS (+) plasmid (Stratagene, USA) for sub-cloning. A resulting clone was further selected and the entire *Eco*RI DNA fragment (E4) was sequenced by the automated DNA sequencing protocol (Takara Korea, Korea).

Computer-assisted sequence and phylogenetic analysis

DNA sequence analysis, translation and alignment with related genes and proteins were carried out using both the computer program Lasergene (DNASTAR, Inc., USA) and ExPASy proteomics server. Homologous genes and proteins were analysed in Basic Local Alignment Search Tool (BLAST) either at National Center for Biotechnology Information (NCBI, http://blast.ncbi.nlm.nih.gov/Blast.cgi) or at network service on ExPASy (http://ca.expasy.org/tools/blast/). Phylogenetic analysis of KatG and Fur-like proteins were performed using the MEGA3 program (*22*) after multiple alignments of the data using the CLUSTAL W program (*23*).

RNA preparation

For transcript analysis, *Mycobacterium* sp. JC1 total RNAs were prepared from the cells grown in SMB-methanol medium at the mid-exponential growth phase by using the RiboPure-Bacteria kit without modification (Ambion, USA). After the final DNaseI inactivation step, the RNA preparation was further cleaned up with the Qiagen RNeasy mini kit (Qiagen, USA) according to the manufacturer's protocol.

Analysis of furA and katG transcripts by RT–PCR

The one-step RT–PCR kit (Qiagen, USA) was used in the *furA* and/or *katG* transcripts analysis. The 25 µl assay contained 7 µl of reaction mix (5 µl of reaction buffer, 1 µl of dNTP mix and 1 µl of E-mix) provided with the kit, 5 U of RNasin (Promega, USA), 1.5 µl of forward and reverse primers (10 uM each) and 100 ng of purified total bacterial RNA. Amplification was carried out in a PCR machine (Eppendorf, USA) as follows: after reverse transcription for 30 min at 50°C, activation for 15 min at 95°C, 35 cycles each of denaturation for 30 s at 94°C, annealing for 30 s at 55°C and elongation for 80 s at 72°C, and then post-elongation was carried out for 10 min at 72°C. The primer sequences and positions used in this study were listed in Table I.

Construction of the plasmid expressing the katG

The entire *katG* coding region of *Mycobacterium* sp. JC1 was amplified by PCR using genomic DNA as a template and the following primer pair based on the *katG* coding sequence found in this study: 5′-CAT*ATGTCATCCGATACGTCC*-3′ (JCP-X5END), consisting of a *Nde*I restriction site (underline) followed by the sequences (italic) encoding the six N-terminal amino acids of JC1 KatG and 5′-CATATG*TCACTTGAGGTCGAACCG*-3′ (JCP-X3END), consisting of the sequences (italic) from final six C-terminal amino acids of JC1 KatG followed by a *Nde*I restriction site (underline). The PCR fragment was directly cloned into pCR2.1 cloning vector (Invitrogen, USA) and the *Nde*I-digested fragment was further cloned into pET-16b expression vector to create pET16-JC1KatG,

Table I. Primers and sequences for detection of *furA-katG* gene and transcript.

Name	Sequence(5′→3′)	Position[a]
F1	GAGACGTGGTATCGATTCGATGGTTG	132–157
F2	ATTCTTGACCGAGTCCAATTCC	204–225
F3	GGCGGTTCTGGAGGCATT	312–329
F4	TCTGCGCCGATTGTGTTG	650–667
F5	TCGACGTGTCACGACTGCAT	865–8B4
F6	GCTGCTCTGGCCTGTCAAAC	1,175–1,194
R1	GTGTCCTCTTCGCCGAACA	1,327–1,345
R2	GATGAACAGGCCGCCATAGT	1,027–1,046
R3	AGTCGTGACACGTCGATCTGAT	858–880
R4	GGTGAGGGCATGAAGAACGT	416–435
R5	GAGGGCATGAAGAACGTCGTA	412–432

[a]All positions are coordinated from the first nucleotide (C) of the E4 DNA fragment (GenBank no. EF421712).

which directed the expression of the recombinant N-terminal His-tag fusion protein with the authentic JC1 KatG sequence.

Expression and purification of His-tagged recombinant KatG protein

pET16-JC1KatG harbouring a complete 2241 bp katG gene was introduced into *E. coli* BL21 (DE3) pLysS and induced by the addition of 1 mM IPTG to cultures at an optical density (A_{600}) of 0.6 at 37°C. After 7 h, the cells were harvested, washed and resuspended in a binding buffer [20 mM potassium phosphate buffer (pH 7.4), 10 mM imidazole and 0.5 M NaCl] and disrupted by sonication. The disrupted cells were centrifuged at 12,000 × *g* for 15 min at 4°C and the resulting cell-free (crude) extract was used for the recombinant KatG protein purification. The purification process was performed using the FPLC system (Pharmacia LKB, USA) equipped with a 5 ml HiTrap chelating HP column (Amersham-Pharmacia Biotech, USA). Of the cell-free extract, 2 ml was applied to the HiTrap column that was pre-equilibrated with the binding buffer and eluted at a flow rate of 2 ml per min with a linear imidazole gradient of 10–500 mM in the binding buffer. Fractions with catalase activity were further analysed by denaturing SDS–PAGE and the fractions with high-purity were combined and desalted using a 5 ml HiTrap desalting column (Amersham Pharmacia Biotech, USA) with 50 mM potassium phosphate buffer (pH 7.0). The desalted fractions were concentrated with a Centricon YM-30 filter unit (Millipore, USA) and used in recombinant KatG characterization.

Catalase and peroxidase activity assays

All assays were carried out at 30°C unless otherwise noted. Catalase activity was assayed using the 50 mM potassium phosphate buffer (pH 7.0) and 12.5 mM H_2O_2 ($\varepsilon_{240} = 43.6\ M^{-1}\,cm^{-1}$) as previously described (*13*). One unit of catalase activity was defined as the amount of enzyme decomposing 1 mmol of H_2O_2 per minute. Standard peroxidase activity was determined by measuring the rate of oxidation of 0.25 mM *o*-dianisidine ($\varepsilon_{460} = 11.3\ mM^{-1}\,cm^{-1}$) in 100 mM citric acid buffer (pH 4.5) with 12.5 mM H_2O_2 as a substrate (*3*). Substrate specificity for the peroxidase activity was determined in 50 mM citric acid buffer (pH 4.5) by following NAD(P)H oxidation at 340 nm ($\varepsilon_{340} = 6.2\ mM^{-1}\,cm^{-1}$), 2,2′-azino-*bis*(3-ethylbenzthiazoline-6-sulphonic acid) (ABTS) oxidation at 414 nm ($\varepsilon_{414} = 36\ mM^{-1}\,cm^{-1}$) or pyrogallol oxidation at 430 nm ($\varepsilon_{430} = 2.47\ mM^{-1}\,cm^{-1}$) using a Beckman DU-70 spectrophotometer. One unit of peroxidase activity was defined as the amount of enzyme that oxidizes 1 μmol of electron donor per min. For the inhibitor and metal ion study, both catalase and peroxidase activities in the purified protein were assayed in the presence of an appropriate chemical in the standard assay mixtures. In order to test stability of the enzyme against organic solvents, the enzyme solution was mixed using vortex with ethanol and chloroform (enzyme solution:ethanol:chloroform = 10:5:3, v/v/v) and left for 30 min at room temperature, followed by measurements of activity. For determining Mn(II) binding to the recombinant KatG protein, the optical absorbance spectra were determined in the Soret region for solutions containing purified recombinant KatG (50 μg ml^{-1}) in 50 mM Tris buffer (pH 8.0) and varying concentrations of $MnSO_4$. The activity staining of KatG was carried out after non-denaturing PAGE by a double staining method for catalase and peroxidase as described previously (*24*).

Nucleotide sequence accession number

The nucleotide sequence reported in this study has been deposited to the GenBank under accession number EF421712.

Results

Cloning of the gene coding for the Mycobacterium sp. JC1 CP protein

Attempts to identify the N-terminal amino acid sequence from the purified *Mycobacterium* sp. JC1 CP were failed possibly due to N-terminal block (*18*). Therefore, a homology-based PCR was carried out to make a probe DNA fragment. A positive cosmid clone (pWEBJCP6-72) was obtained by colony lift hybridization of the *Mycobacterium* sp. JC1 genomic cosmid library with the DIG-labelled probe (JCP-probe) synthesized based on the PCR product of two JCP-F/-R primers. Southern hybridization of the cosmid clone revealed that the probe hybridized to one each of *Bgl*II (5.5 kb), *Eco*RI (5.8 kb), *Hind*III (5.3 kb) and *Sma*I (>10 kb) fragments (data not shown). The 5.8 kbp *Eco*RI fragment was subcloned into pBluescript vector and the corresponding *Eco*RI fragment (E4) was completely sequenced.

The nucleotide sequence analysis of the E4 fragment showed that it consisted of 5,706 nucleotides and the overall GC content was 65.7%, representing a characteristic high GC content of mycobacterial genome. The deduced amino acid sequence analysis and the BLAST similarity search of the E4 fragment revealed the presence of several potential ORFs. A 2,241-bp ORF from the initiation codon ATG to the termination codon TGA showed high homology to mycobacterial KatG proteins. Another putative ORF revealed the presence of two potential start codons beginning at different ATG (coordination 151 of E4) and GTG (coordination 244 of E4) but the translation stop codon ending at the same TGA (coordination 679 of E4). A 438 bp ORF starting with the GTG codon showed high homology to Fur-like proteins. Besides the two putative FurA and KatG ORFs, there was an N-terminus truncated ORF at coordination 5706 to 4609 in the opposite direction of the *furA–katG* transcription showing a 50% identity to the putative adenylate cyclases (CyaA) of *M. smegmatis*, *M. avium* and *M. tuberculosis* (data not shown). Figure 1 represented the restriction map of the E4 DNA fragment based on the entire sequencing results and transcriptional directions of the three putative ORFs.

Annotation of Mycobacterium sp. JC1 KatG and FurA genes

The putative *katG* gene at coordination 720 to 2960 of E4 could code for a protein of 746 amino acid residues. The calculated molecular mass and pI of the protein were 81,748 Da and 4.94, respectively. A potential Shine–Dalgarno (SD) sequence (GAAG GA) was present 6 bp upstream of the ATG initiation codon. BLAST similarity search showed that the

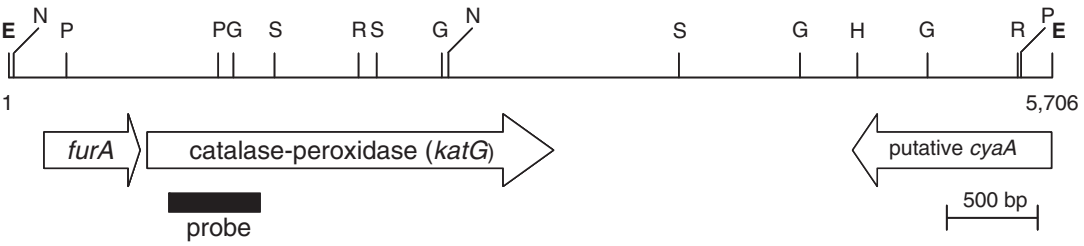

Fig. 1 Restriction map of the 5.7 kb *Eco*RI fragment (E4) containing the *Mycobacterium* sp. JC1 *furA* and *katG* genes. Thick arrows indicate the directions and positions of the *furA*, *katG* and *cyaA* genes. The JCP probe binding site for southern hybridization is depicted as a black bar. Abbreviations for restriction enzymes: E, *Eco*RI; G, *Bgl*II; H, *Hind*III; N, *Not*I; P, *Pvu*II; R, *Eco*RV; S, *Sac*I.

```
JC1   VPHSAHFREQLREADLRVTQPRVAVLEALV..AHPHADTETIFSAVRDTLPNVSRQAIYDVLHALTTAHLIRRIQPSGSSARYE   82
MSM   MPSRAEFEAQLRMTDLRVTRPRIAVMEAVH..ANPHADTETIYSVVRGSLPTVSRQAVYDVLHALTAANLVRRIQPSGATARYE   82
MAV              MADLRVTRPRVAVLEVVD..ANPHADTETIFSAVRMALPDVSRQAVYDVLNALTAVGLVRRIQPLGMVARYE   70
MTB   MSSIPDYAEQLRTADLRVTRPRVAVLEAVN..AHPHADTETIFGAVRFALPDVSRQAVYDVLHALTAAGLVRKIQPSGSVARYE   82
MFO   MADGLDFTGMLRSAGLRITRPRLAVLNAVK..EHPHAETDHVIRAVRVQLPDVSHQTVYDXLNALTAAGLVRRIQPTGSVARYE   82
ECO      MTDNNTALKKAGLKVTLPRLKILEVLQEPDNHHVSAEDLYKRLIDMGEEIGLATVYRVLNQFDDAGIVTRHNFEGGKSVFE   81
                :. :.*::*.** :::::.    . :*:::::.  .::  :: ::.:.:*::* :::.:.:::::::: *  :::*

                HXHXXCXXC                                                  C pair
JC1   SRVGDNHHHVVCRGCRAIADVDCAVGAAPCLTPS.DDAALDGFVLDEAEVIYWG.........FCA..DCVAASP          145
MSM   ARVGDNHHHVVCRNCGSIADVDCAVGEAPCLTPSNDDHALDGFLLDEAEVIYWG.........RCR..ECSVDGP          146
MAV   SRVGDNHHHVVCRSCGTIADVDCAVGEAPCLTPSDDDNVLDGFVLDEAEVIYWG.........LCA..DCSTAGS          134
MTB   SRVGDNHHHIVCRSCGVIADVDCAVGEAPCLTAS....DHNGFLLDEAEVIYWG.........LCP..DCSISDTSRSHP      147
MFO   TRVNDNHHHVVCRSCGAIADVDCAVGDAPCLTAADD....NGFDIDEAEVIYWASALTARDLRVLD..DSPVAHQMKGKAMPPNT 161
ECO   LTQQHHHDHLICLDCGKVIEFSDDSIEARQREIAAK....HGIRLTNHSLYLYG.........HCAEGDCREDEHAHEGK      148
       ::.::*:*.:*: *: ::::::::::.*:::: . .     *: ::::::::::          :   ::
```

Fig. 2 Comparison of the predicted amino acid sequence of the *Mycobacterium* sp. JC1 FurA with those of other Fur homologues. The compared Fur homologues are *Mycobacterium* sp. JC1 (JC1; ABO09796), *M. smegmatis* mc^2-155 (MSM; ABK74841), *M. avium* 104 (MAV; ABK69390), *M. tuberculosis* H37Rv (MTB; AAB63370), *M. fortuitum* (MFO; CAA76608) and *E. coli* K-12 (ECO; X02589). Asterisks and dots indicate identical and similar amino acids, respectively. The residue numbers are shown on the right. Conserved HXHXXCXXC motif and C (cysteine) pair are noted above the JC1 FurA sequence. Identical residues among mycobacterial FurAs are underlined in the MTB FurA sequence.

putative sequence had overall identities exceeding 70% with other mycobacterial KatGs including *M. tuberculosis* and had the highest identity of over 86% to *M. smegmatis* KatG2 (GenBank accession no. ABK73887) (data not shown). Multiple alignments with other mycobacterial KatGs showed that the important distal [Arg-104, Trp-107 and His-108 residues; all coordinates are for *M. tuberculosis* KatG (GenBank accession no. X68081)] and proximal (His-270, Trp-321, and Asp-381 residues) residues in haem binding pocket (*25*, *26*) for enzyme activity were well conserved in the *Mycobacterium* sp. JC1 putative KatG. Also, the important residues (Asp-137, Tyr-229, Val-230, Asn-231, Pro-232 and Ser-315) for INH binding and activation (*25*, *27*) were invariant between JC1 and other mycobacterial KatGs.

The putative 438-bp *furA* ORF from the GTG initiation codon could encode a polypeptide of 145-amino-acids with a calculated molecular mass of 15,720 Da and a pI of 5.62. Between the putative *furA* stop codon TGA and the putative *katG* start codon ATG, there was a 38 bp gap space. The putative FurA had comparable similarities with other mycobacterial FurAs (78–85%) and *M. avium* 104 FurA (GenBank accession no. ABK69390) showed the highest identity with the putative JC1 FurA (79%) (data not shown). Alignment analysis with other Fur-like proteins revealed that a HXHXXCXXC motif that is likely to participate in binding metals was conserved in the putative FurA and that an additional cysteine (C) pair near the C terminus was also conserved among the Fur proteins compared (Fig. 2).

Phylogenetic analysis of KatG and FurA proteins

Phylogenetic analysis of the putative KatG using the MEGA3 program revealed that the JC1 KatG was the closest relationship with KatG2 of *M. smegmatis* mc^2-155 (GenBank accession no. ABK73887). It also clustered with KatG proteins from other bacterial species including *E. coli*, but not with the typical catalase proteins from other bacterial and fungi species having the resistance of organic solvents (Fig. 3A).

The putative JC1 FurA protein also showed the closest relationship with Fur2 protein of *M. smegmatis* mc^2-155 (GenBank accession no. ABK74841) in a phylogenetic tree. And it clustered with the other mycobacterial Fur proteins, but not with *E. coli* Fur protein (Fig. 3B).

Analysis of the furA and katG transcription

The position of the JC1 *furA*, situated 38 bp upstream of the putative *katG*, suggests that the two genes could be co-transcribed. To define the transcriptional organization of the *furA* and *katG*, we had tried primer extension analysis with 24-mer (R5) and 26-mer (R3, shown in Fig. 4A and Table I) synthetic primers that are complementary to nucleotide positions

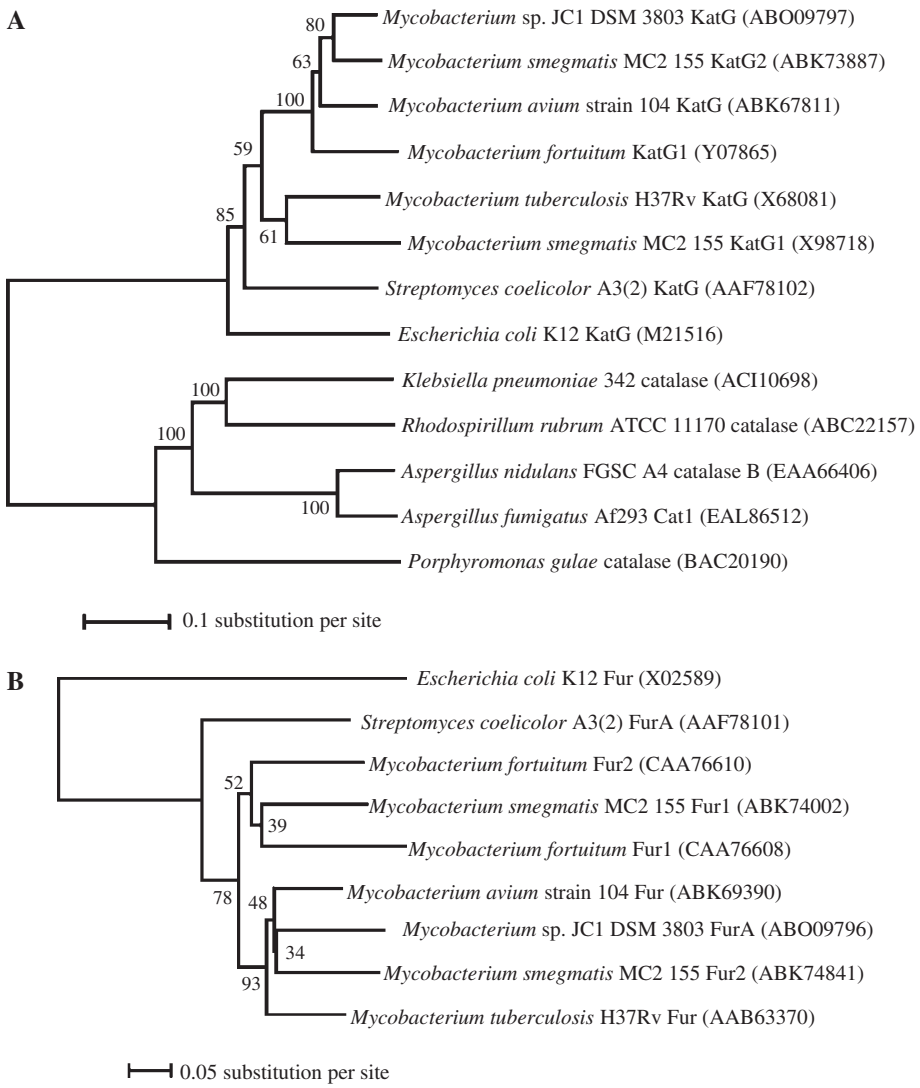

Fig. 3 Phylogenetic trees of the deduced protein sequences of KatG (A) and Fur-like (B) proteins. Amino acid sequence alignments were performed using CLUSTAL W. The tree was generated by neighbour-joining (Poisson correction model) using the MEGA 3 program. The gaps in the alignment were completely deleted. The GenBank accession numbers for the sequences were given in parentheses. Bootstrap values were calculated from 100 replicates. KatG, catalase–peroxidase; Fur, ferric uptake regulator.

169–192 and 140–165 downstreams of the *furA* GTG and the *katG* ATG start codons, respectively. However, we could not map the 5′ ends of the transcripts. Alternatively, we employed an RT–PCR mapping strategy for finding *Mycobacterium* sp. JC1 *furA* and/or *katG* transcripts. From a routine PCR strategy with primers listed in Table I, the DNA fragments proposed in Fig. 4A were clearly amplified from the genomic DNA extracted from *Mycobacterium* sp. JC1 (Fig. 4B, PCR), indicating that the designed primers could be used for this experimental purpose. From the one-step RT–PCR protocol with F1/R4 primer pairs and the total RNAs extracted from *Mycobacterium* sp. JC1 as templates, a fragment extending from positions −19 to +285 relative to the ATG start codon of *fur*A was clearly amplified (see lane 2 in Fig. 4B, RT–PCR). However, an RT–PCR combination with the F1/R3 primers, which were situated at positions from −19 to +730 (inside *kat*G region) relative to the ATG start codon of the *fur*A, did not amplify any fragments (see lane 3 in Fig. 4B, RT–PCR). An RT–PCR analysis for the *kat*G transcript with the F4/R1 primers situated at positions −70 to +626 relative to the ATG start codon of the *kat*G revealed that the 5′ end of the katG transcript lay near in 70 bp upstream region from the *kat*G start codon ATG (see lane 8 in Fig. 4B, RT–PCR). Further RT–PCR analysis using reverse primers covering the downstream region of the *fur*A stop codon TGA showed that the JC1 *fur*A transcription terminated in the region between the *fur*A stop codon TGA and the *kat*G initiation codon ATG (data not shown). Taken together, the RT–PCR results suggest that the *kat*G is not co-transcribed with the *fur*A.

Overproduction and purification of the putative KatG protein in E. coli

The putative KatG protein of *Mycobacterium* sp. JC1 was overproduced in *E. coli* using the pET-16b expression system. The recombinant KatG protein

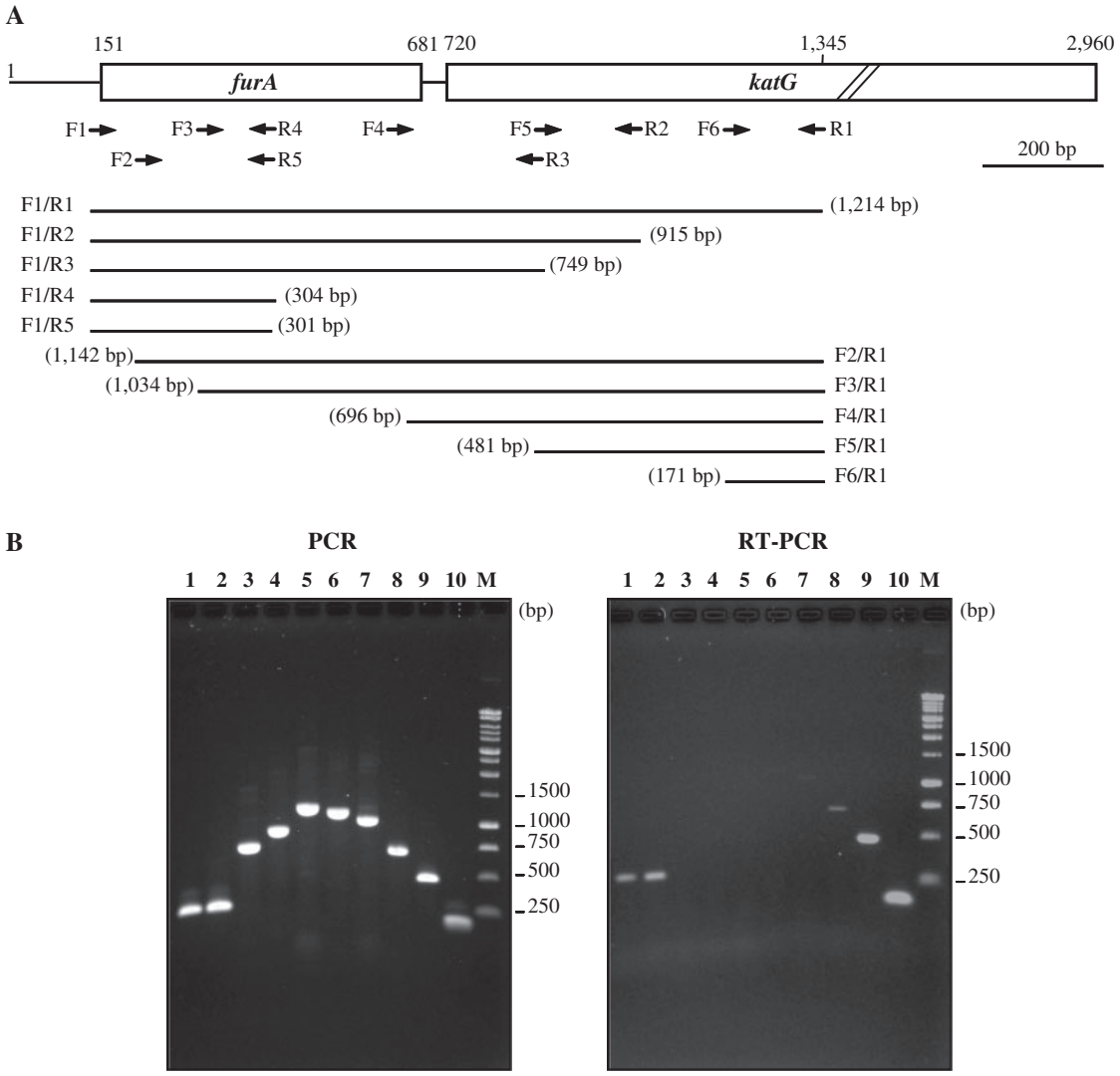

Fig. 4 Analysis of the *Mycobacterium* sp. JC1 *furA* and *katG* transcripts by RT–PCR. (A) Schematic representation of PCR and RT–PCR strategies. The *furA–katG* region of *Mycobacterium* sp. JC1 is drawn to scale according to the E4 DNA fragment sequence (Genbank accession no. EF421712). The numbers are coordinated from the first nucleotide (C) of the E4 DNA fragment. The genes are indicated by boxes. The names, positions and directions (arrows) of the primers are reported. The primer pairs and the expected sizes of the amplified products are also shown. (B) PCR and RT–PCR results. PCR and RT–PCR were performed with the primer pair of F1/R5 (lane 1), F1/R4 (lane 2), F1/R3 (lane 3), F1/R2 (lane 4), F1/R1 (lane 5), F2/R1 (lane 6), F3/R1 (lane 7), F4/R1 (lane 8), F5/R1 (lane 9) and F6/R1 (lane 10) using JC1 genomic DNA (PCR) and JC1 total RNAs (RT–PCR) as templates, respectively. M: benchtop 1 kb DNA ladder (Promega, USA).

was not only highly expressed as a soluble form but it was also expressed as insoluble inclusion bodies depending on culture time after IPTG induction (data not shown). Therefore, the cells were collected in 6–10 h after IPTG treatment and used to purify the recombinant protein with Ni-NTA affinity column chromatography.

The affinity-purified recombinant protein fraction after desalting and concentration steps showed a major band with a molecular weight of 82 kDa and some minor bands on a 12.5% denaturing polyacrylamide gel (Fig. 5), indicating that the estimated purity of the major band was ~90% homogeneity. Double activity staining revealed that the major band had both catalase and peroxidase activities. Western blot analysis revealed that the recombinant protein was clearly recognized by the antiserum raised against the purified native JC1 CP (*18*) (data not shown).

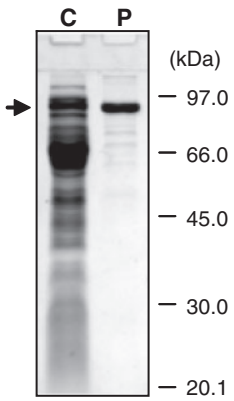

Fig. 5 Overproduction of the recombinant *Mycobacterium* sp. JC1 KatG proteins in *E. coli*. An SDS–PAGE (12.5% acrylamide) was performed with cell-free extract (C; 40 μg) and the purified recombinant protein (P; 7.6 μg). After gel electrophoresis, the gel was subjected to Coomassie brilliant blue staining. The overproduced recombinant JC1 KatG was indicated with an arrow.

Table II. Comparison of biochemical properties between native and recombinant KatGs of *Mycobactrium* sp. JC1

	Native KatG[a]		Recombinant KatG	
Properties	Catalase	Peroxidase	Catalase	Peroxidase
Biochemical properties				
Optimal temperature	40°C	30°C	40°C	4O°C
Optimal pH	7.0	4.0	7.0	4.0–4.5
Catalase activity	1.15 U/mg	–	1.03 U/mg	–
o-dianisidine oxidation	–	3.48 U/mg	–	3.3 U/mg
K_m (H_2O_2)	6.3 mM	1.47 mM	2.05 mM	2.1 mM
Inhibitors[b]			1	1
Hydroxylamine (0.1 mM)	1%	83%	1%	92%
NaN_3 (1 mM)	8%	1%	7%	1%
KCN (1 mM)	4%	4%	1%	1%
Mn ion (1 mM)	ND[c]	ND	53%	38%
Other properties				
Resistance to organic solvents[d]	90%	90%	82%	84%
Sonet peak	406 nm		407 nm	

[a]Data shown here were from the previous publication (*18*). [b]Activities in the absence of inhibitor were set as 100%. [c]not determined. [d]Activities in the absence of organic solvents were set as 100%.

Characterization of the recombinant KatG protein

The catalase activity of the purified recombinant KatG protein was 1.03 U mg^{-1}, similar to that of the native JC1 CP (1.15 U mg^{-1}). The peroxidase activity of the KatG protein exhibited a broad range of substrate specificity including NADH (0.84 U mg^{-1}), NADPH (0.69 U mg^{-1}), *o*-dianisidine (3.3 U mg^{-1}), ABTS (1.1 U mg^{-1}) and pyrogallol (2.9 U mg^{-1}). The spectral properties of the purified protein exhibited a typical Soret band at 407 nm (data not shown), indicating that it is a ferric haem-containing protein, like the native JC1 CP (*18*). However, the apparent K_m values of H_2O_2 for both catalase and peroxidase activities on the recombinant KatG protein were 3-fold lower and 0.5-fold higher than those on the native KatG protein, respectively (Table II).

With regard to the effects of organic solvents, the recombinant KatG retained up to 82 and 84% of their initial catalase and peroxidase activities (0.85 U mg^{-1} and 2.77 U mg^{-1}, respectively) after incubation with ethanol–chloroform mixtures for 30 min (Table II). This demonstrates the marked resistance of *Mycobacterium* sp. JC1 KatG to organic solvents, even though the recombinant KatG exhibited ~10% less resistance against organic solvent than the native KatG protein. As summarized in Table II, therefore, biochemical and physical properties of the recombinant KatG were almost identical to those of the native JC1 CP previously reported (*18*), indicating that the native CP and the recombinant KatG are indistinguishable.

Inhibitor study on the recombinant KatG activity showed that most of the catalase activity (99%) was inhibited by 0.1 mM hydroxylamine treatment (Table II). However, even 10-fold more excess of hydroxylamine (1 mM) was required to inhibit only 60% of the peroxidase activity (data not shown). Interestingly, inhibition patterns of KatG activity by isoniazid (INH) and dithiothreitol (DTT) were totally opposite to those by hydroxylamine. INH inhibited most of the peroxidase activity at 0.1 mM concentration (96% reduction), but similar inhibition of the catalase activity was achieved by over 1 mM (76% reduction) of INH treatment. DTT also completely abolished the peroxidase activity at 1 mM, but it had no effect on the catalase activity at the same concentration (data not shown).

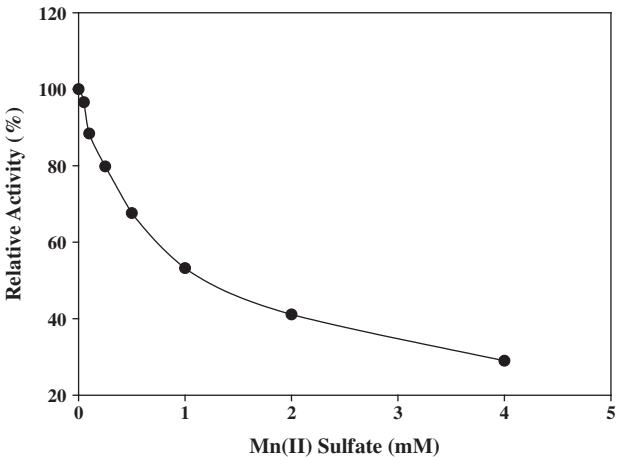

Fig. 6 Dose-dependent inhibition of Mn(II) on the catalase activity of the recombinant KatG protein. The catalase activity was measured in the reaction mixture [50 mM Tris buffer (pH 8.0) and 12.5 mM H_2O_2] with different concentrations of $MnSO_4$. The activity in the absence of Mn(II) was set as 100%.

Interestingly, among some divalent metal ions tested, manganese ion revealed some inhibitory effects on the recombinant KatG activity. Of the peroxidase activity, 62% was inhibited by 1 mM of manganese ion, but 26% of this inhibition was relieved by an addition of 1 mM EDTA (data not shown). Also the catalase activity of the recombinant KatG protein was dose-dependently inhibited by manganese (II) sulphate (Fig. 6) and the K_i for Mn(II) calculated from these rates was 0.89 mM (data not shown), suggesting the involvement of Mn(II) on the KatG activity. An evidence for manganese binding to the catalase–peroxidase enzyme was supplied by spectroscopic

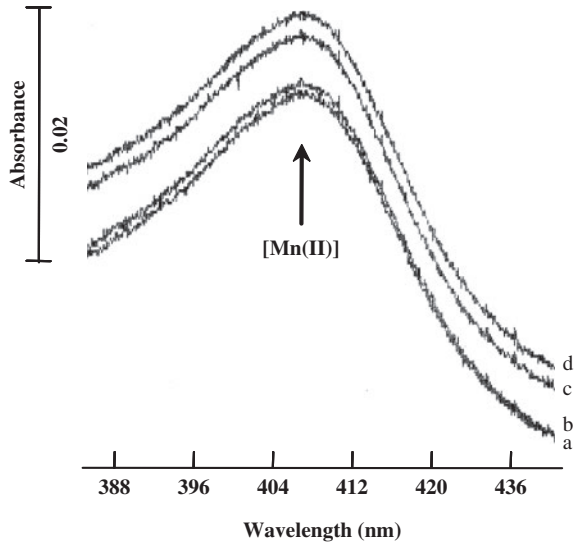

Fig. 7 Spectroscopic titration of the purified recombinant KatG with Mn(II). Absolute spectra were determined for solutions containing the purified recombinant KatG (50 μg ml^{-1}) in 50 mM Tris buffer (pH 8.0) and varying concentrations of $MnSO_4$: 0 μM (a); 50 μM (b); 100 μM (c) and 200 μM (d).

analysis. The addition of Mn(II) to the enzyme solution showed the small change in intensity of the Soret absorbance at 407 nm (Fig. 7), indicating that Mn(II) binds to near the haem of the JC1 KatG protein.

Discussion

KatG is a unique dual function enzyme acting as catalase and peroxidase. These enzymatic activities are important for protection against damage from reactive oxygen species (*28*). In addition, *M. tuberculosis* KatG is the enzyme responsible for activation of the anti-tuberculosis drug INH and its mutations are the primary source of drug resistance in clinical strains. In spite of vast investigations to reveal the relationship between the enzyme structure and activity, the exact mechanisms of the dual-function of the enzyme and INH activation are not well known. For these reasons, KatGs with various origins have been cloned and their enzyme kinetics have been extensively examined.

The deduced amino acid sequence of the JC1 *katG* gene had high identity with other mycobacterial KatGs and essential motifs for KatG activity and INH activation were also well conserved. The deduced molecular mass and pI of the KatG protein were 81.7 kDa and 4.9, respectively. This is in good agreement with those of the native JC1 CP (80 kDa and 4.8, respectively) previously calculated (*18*). The *furA*-like gene, which is located only 38 bp upstream of the *katG* showed also a high identity with other mycobacterial FurAs. Although sequence analysis initially predicted that the *furA* ORF could start from coordination 151 bp of the E4 sequence with methionine (ATG) for a start codon, multiple alignment analysis revealed that an additional 31 amino acid in the N-terminal region of the predicted JC1 FurA did match neither to other mycobacterial FurAs nor to unrelated bacterial Fur proteins suggesting that a more distal GTG codon (coordination 244–246 bp of E4) could be an alternative start codon. Since a putative SD sequence (GAAGG) is found in the 12 bp upstream of the GTG codon, the GTG codon has a possibility to be a translation start codon for the JC1 FurA protein. Currently, we are overproducing the FurA protein in *E. coli* for generating the FurA polyclonal antibody. Western blot analysis using this antibody will give us a clue whether the GTG is the translation initiation codon for the FurA expression.

The *furA–katG* clustering seems to be a characteristic feature of the order *Actinomycetales*, including the genus *Mycobacterium* and *Streptomyces* (*29*, *30*). *M. smegmatis* contains three paralogues of *katG* in a completely sequenced genome available at Comprehensive Microbial Resource (CMR) of The Institute for Genomic Research (TIGR) (*31*). Among the three *katG* gene loci of *M. smegmatis*, only two loci have *furA* in the upstream region respective to *katG* genes (TIGR annotation for *furA–katG* cluster: MSMEG_3460-MSMEG_3461 and MSMEG_6383-MSMEG_6384). All the other mycobacteria of which full genome sequences are available show only one *furA–katG* cluster in their genome including *M. bovis* and *M. tuberculosis*. Phylogenetic analysis suggests that JC1 *furA–katG* is more closely related to first cluster *furA–katG* of *M. smegmatis* [MSMEG_3460 (or ABK74841) and MSEMG_3461 (or ABK73887)]. In contrast, *M. tuberculosis furA–katG* locus is more similar with the second cluster of *M. smegmatis* [MSEMG_6383 (or ABK74002) and MSEMG_6384 (or X98718)].

Promoter prediction analysis for the prokaryotic gene sequence through web-based Promoter Finder program (http://www.fruitfly.org/seq_tools/promoter.html) predicted the T residue at 71 nucleotides upstream from the KatG initiation codon ATG as a transcriptional start site for the *katG* transcript. Upstream of the transcription start point, −35 (TGT ACT) and −10 (TATCTA) consensus sequences are also found. However, there are no possible promoter regions predicted in upstream of the putative *furA* ORF. Our attempts to map the transcriptional start sites of the *furA* and *katG* genes through primer extension analysis, based on the prediction analysis above, were unsuccessful. The reasons are uncertain, but probably due to the complicated RNA secondary structure formed in the 5′ end of the *furA* and *katG* transcripts. Instead, using RT–PCR experiments with JC1 total RNAs, we found that a transcript covering both *furA* and *katG* was not formed, suggesting the two genes are not co-transcribed. Although we could not precisely map the transcription start sites for the *furA* and *katG* transcripts, our RT–PCR experiments presume that the *furA* transcription starts at the upstream region of the GTG initiation codon and ends in the upstream region of the ATG initiation codon for KatG protein. Also, the *katG* transcription presumably starts in at least 70 bp upstream region from the KatG initiation codon ATG. It is in good correlation with the promoter prediction analysis, presuming that the predicted T nucleotide is presumably the

transcription start point for the *Mycobacterium* sp. JC1 *katG* gene. Taken together, we conclude that *Mycobacterium* sp. JC1 *katG* is independently transcribed from the *furA*, similar to *M. smegmatis*, which shows independent transcription of the *furA* and *katG* genes (*29*). However, S1 nuclease protection study showed that the two genes are co-transcribed in *M. tuberculosis* (*32*, *33*), indicating that transcriptional regulations of the two genes may vary among mycobacteria.

The conserved *furA–katG* locus in mycobacteria suggests that FurA may control KatG expression. Indeed, the mycobacterial *furA* have demonstrated that it is a negative regulator of its *katG* (*34*). The presence of an oxidative stress-responsive promoter, immediately upstream of the *furA* gene, has been reported previously for *M. tuberculosis*, *M. smegmatis* and *M. bovis* BCG (*29*, *32*, *33*). Sequence analysis of the promoters revealed that a 23 bp AT-rich sequence, overlapping the −35 region of *furA* promoter (*pfurA*), was identified and found to be conserved among mycobacteria (*35*). Gel shift and foot-printing analysis further revealed that the AT-rich sequence in *M. tuberculosis pfurA* was essential for the FurA binding and peroxide treatment of the FurA abolished DNA binding, confirming that *M. tuberculosis* FurA expression is regulated by its own oxidative stress-responsive promoter (*pfurA*) (*35*). The 23 bp AT-rich sequence of *pfurA* is not, however, conserved in the *Mycobacterium* sp. JC1 *furA* promoter region. Therefore, we do not know whether the *Mycobacterium* sp. JC1 FurA protein autoregulates its own expression and its promoter is an oxidative stress-responsive promoter, yet.

Recently, it has been reported that the *katG* mRNA of *M. tuberculosis* or *M. smegmatis* is processed at their 5′ end and it is stabilized by both a polypurine sequence (PPS) and translation initiation (*36*). The transcribed mRNA is immediately processed and this processing is prevented by a double-stranded RNA at the cutting site, suggesting an involvement of the single-strand cutting endoribonuclease. The PPS (GG AAGGAA) four bases upstream of the KatG translation start codon in *M. tuberculosis* and *M. smegmatis*, which is similar to the SD sequence, is also found in four bases upstream of the KatG translation start codon in *Mycobacterium* sp. JC1 (GGAAG GA). However, it remains unsolved whether these processing and/or stabilization events also occur in *Mycobacterium* sp. JC1. It is likely that future studies regarding to those questions mentioned above will provide insights into mechanisms of the *Mycobacterim* sp. JC1 *furA* and *katG* transcriptional and translational regulation.

Despite the fact that the recombinant JC1 KatG overproduced in *E. coli* showed very similar physical and biochemical properties with the native JC1 CP (see Table II for details), there were some differences in the apparent K_m values of H_2O_2 for both catalase and peroxidase activities on the recombinant KatG protein. It indicates that the native and recombinant KatG proteins show some differences in substrate binding affinity. We did not further examine the reason, but it could be due to a slight structural difference of the recombinant KatG protein caused probably by the addition of 6-histidine residues in the C-terminus.

Among the properties examined here, it is interesting that manganese showed some inhibitory effects on the JC1 KatG activity and the inhibition could be relieved by EDTA. This implies that manganese may competitively bind to near the haem group and involve in the enzyme reaction. Direct evidences for Mn(II) binding near the haem of resting (ferric) enzymes have been reported by difference spectroscopy when the enzymes were titrated with Mn(II) (*37*, *38*). In the case of *Mycobacterium* sp. JC1 KatG enzyme, the small change in the intensity of the Soret absorbance at 407 nm (0.005 absorbance units), which was complete upon the addition of 100 μM Mn(II), was also found. And it was similar to those reported for the ferric enzymes (manganese peroxidase and catalase–peroxidase) (*37*, *38*), demonstrating manganese binding to the JC1 KatG enzyme. Manganese is known to be involved in several catalase and peroxidase activities, independent of the absence or presence of the haem group. Pseudo-catalases independent of the haem-iron structure are manganese-containing enzymes (*39–41*). *Streptomyces reticuli* catalase–peroxidase CpeB has the haem-independent manganese peroxidase activity, because its haem apo-form catalyses the peroxidation of Mn(II) to Mn(III) (*42*). Also, haem-containing fungal manganese peroxidases (MnPs) oxidize a variety of organic compounds but only in the presence of Mn(II) (*43*, *44*). The crystal structure study of MnP shows that three acidic amino acids (Glu^{35}, Glu^{39} and Asp^{179}) and the haem proprionate are involved in Mn(II) binding (*45*). Moreover, the catalase–peroxidase of *M. smegmatis* exhibits Mn(II)-peroxidase activity and its Mn(II) binding occurs near the haem of resting (ferric) protein (*38*). Since the JC1 KatG is very closely related to *M. smegmatis* KatG in the phylogenetic analysis, we suggest that Mn(II) binds near the haem of the JC1 KatG protein and the enzyme catalyses the peroxidation of manganese ion, similar to the *M. smegmatis* KatG (*44*).

Another interesting fact is that the JC1 KatG is stable when treated with ethanol/chloroform. This resistance of organic solvent is a property of true catalase, but not of catalase–peroxidase (*46–49*). The phylogenetic analysis shows that the catalase–peroxidase (KatG) proteins including the JC1 KatG have evolved independently from the catalase proteins showing ethanol/chloroform resistance and form a discrete phylogenetic group. This implies that the JC1 KatG is truly one of the KatG family proteins and it is notably stable in ethanol/chloroform treatment. It remains, however, to be solved why the JC1 KatG reveals some resistance of organic solvents.

On the other hand, INH and DTT selectively affected the peroxidase activity rather than catalase activity at the same concentration. It is reported that the most obvious access route to the distal side of the haem, the active site of the enzyme for reaction with H_2O_2, is provided by a channel positioned similarly to, but longer and more constricted than, the access route

in other haem peroxidases (*50*). INH occupation of the active site or channel may hinder peroxidase activity with sparing catalase activity. It is also possible that the peroxidase activity depends on disulphide bonds, since DTT reduces and cleaves disulphide bonds and it may preferentially abolish the peroxidase activity. Because the JC1 KatG pretreated with β-mercaptoethanol lost the peroxidase activity, but not the catalase activity (data not shown), it implies that cysteine residues and disulphide bonds for the KatG dimer formation are important in peroxidase activity and possibly INH activation.

In spite of a great similarity with *M. tuberculosis* KatG in the amino acid sequence, *Mycobacterium* sp. strain JC1 reveals INH resistance (*18*). Critical enzymatic active sites and key residues for INH binding and activation are conserved in well-known mycobacterial KatGs and JC1 KatG. Especially the 315th serine residue (based on *M. tuberculosis* KatG coordination), which is the most frequently changed to threonine in INH-resistant *M. tuberculosis* (*51*), is also conserved in JC1 KatG. This implies that the other critical residues that are attributed to INH activation may differ among pathogenic and non-pathogenic mycobacteria. One of such candidates can be a couple of N-terminal residues, tyrosine-28 and tryptophan-38 in *M. tuberculosis* KatG, which are important for homodimer formation as a 'hook' revealed by a crystal structure study (*25*). These residues are not conserved in JC1 KatG. It is also possible that INH binding and activation sites are intact in JC1 KatG, but some target enzymes (InhA and KasA) are activated by INH are different among mycobacteria (*52*).

In this study, we show that JC1 recombinant KatG overproduced in *E. coli* is as intact as the native enzyme. The robust yield of the recombinant protein and the easy purification of it will facilitate the structural study of JC1 KatG for finding functional domains of Mn(II) binding and enzyme properties. Also, more detailed alignment analysis of the amino acid sequence of the JC1 KatG protein together with other ethanol/chloroform-resistant catalase proteins and mutant study could provide some important insights into the resistance of organic solvent in the related enzyme.

Funding

Korea Science and Engineering Foundation (KOSEF) grant funded by the Korea government (MEST) (Grant No. R01-2008-000-12139-0).

Conflict of interest

None declared.

References

1. Faguy, D.M. and Doolittle, W.F. (2000) Horizontal transfer of catalase–peroxidase genes between archaea and pathogenic bacteria. *Trends Genet*. **16**, 196–197
2. Pongpom, P., Cooper, C.R. Jr., and Vanittanakom, N. (2005) Isolation and characterization of a catalase–peroxidase gene from the pathogenic fungus, *Penicillium marneffei*. *Med. Mycol*. **43**, 403–411
3. Hochman, A. and Goldberg, I. (1991) Purification and characterization of a catalase–peroxidase and a typical catalase from the bacterium *Klebsiella pneumoniae*. *Biochim. Biophys. Acta* **1077**, 299–307
4. Claiborne, A. and Fridovich, I. (1979) Purification of the o-dianisidine peroxidase from *Escherichia coli* B. Physicochemical characterization and analysis of its dual catalatic and peroxidatic activities. *J. Biol. Chem*. **254**, 4245–4252
5. Marcinkeviciene, J.A., Magliozzo, R.S., and Blanchard, J.S. (1995) Purification and characterization of the *Mycobacterium smegmatis* catalase–peroxidase involved in isoniazid activation. *J. Biol. Chem*. **270**, 22290–22295
6. Johnsson, K., Froland, W.A., and Schultz, P.G. (1997) Overexpression, purification, and characterization of the catalase–peroxidase KatG from *Mycobacterium tuberculosis*. *J. Biol. Chem*. **272**, 2834–2840
7. McDonough, K.A., Kress, Y., and Bloom, B.R. (1993) Pathogenesis of tuberculosis: interaction of *Mycobacterium tuberculosis* with macrophages. *Infect. Immun*. **61**, 2763–2773
8. Manca, C., Paul, S., Barry, C.E. III, Freedman, V.H., and Kaplan, G. (1999) *Mycobacterium tuberculosis* catalase and peroxidase activities and resistance to oxidative killing in human monocytes *in vitro*. *Infect. Immun*. **67**, 74–79
9. Zhao, X., Yu, H., Yu, S., Wang, F., Sacchettini, J.C., and Magliozzo, R.S. (2006) Hydrogen peroxide-mediated isoniazid activation catalyzed by *Mycobacterium tuberculosis* catalase–peroxidase (KatG) and its S315T mutant. *Biochemistry* **45**, 4131–4140
10. Zhang, Y., Heym, B., Allen, B., Young, D., and Cole, S. (1992) The catalase–peroxidase gene and isoniazid resistance of *Mycobacterium tuberculosis*. *Nature* **358**, 591–593
11. Heym, B., Alzari, P.M., Honore, N., and Cole, S.T. (1995) Missense mutations in the catalase–peroxidase gene, *katG*, are associated with isoniazid resistance in *Mycobacterium tuberculosis*. *Mol. Microbiol*. **15**, 235–245
12. Kim, K.S., Ro, Y.T., and Kim, Y.M. (1989) Purification and some properties of carbon monoxide dehydrogenase from *Acinetobacter* sp. strain JC1 DSM 3803. *J. Bacteriol*. **171**, 958–964
13. Ro, Y.T., Seo, J.G., Lee, J., Kim, D., Chung, I.K., Kim, T.U., and Kim, Y.M. (1997) Growth on methanol of a carboxydobacterium, *Acinetobacter* sp. strain JC1 DSM 3803. *J. Microbiol*. **35**, 30–39
14. Park, S.W., Hwang, E.H., Park, H., Kim, J.A., Heo, J., Lee, K.H., Song, T., Kim, E., Ro, Y.T., Kim, S.W., and Kim, Y.M. (2003) Growth of mycobacteria on carbon monoxide and methanol. *J. Bacteriol*. **185**, 142–147
15. Lee, H.I., Kim, Y.M., and Ro, Y.T. (2008) Purification and characterization of a copper-containing amine oxidase from *Mycobacterium* sp. strain JC1 DSM 3803 grown on benzylamine. *J. Biochem*. **144**, 107–114
16. Shin, K.J., Ro, Y.T., and Kim, Y.M. (1994) Catalases in Acinetobacter sp. strain JC1 DSM 3803 growing on glucose. *Kor. J. Microbiol*. **32**, 155–162
17. Ro, Y.T., Kim, E., and Kim, Y.M. (2000) Enzyme activities related to the methanol oxidation of *Mycobacterium* sp. strain JC1 DSM 3803. *J. Microbiol*. **38**, 209–217
18. Ro, Y.T., Lee, H.I., Kim, E.J., Koo, J.H., Kim, E., and Kim, Y.M. (2003) Purification, characterization, and

physiological response of a catalase–peroxidase in *Mycobacterium* sp. strain JC1 DSM 3803 grown on methanol. *FEMS Microbiol. Lett.* **226**, 397–403
19. Kim, Y.M. and Hegeman, G.D. (1981) Purification and some properties of carbon monoxide dehydrogenase from *Pseudomonas carboxydohydrogena*. *J. Bacteriol.* **148**, 904–911
20. Goldberg, J.B. and Ohman, D.E. (1984) Cloning and expression in *Pseudomonas aeruginosa* of a gene involved in the production of alginate. *J. Bacteriol.* **158**, 1115–1121
21. Zamocky, M., Regelsberger, G., Jakopitsch, C., and Obinger, C. (2001) The molecular peculiarities of catalase–peroxidases. *FEBS Lett.* **492**, 177–182
22. Kumar, S., Tamura, K., and Nei, M. (2004) MEGA3: Integrated software for Molecular Evolutionary Genetics Analysis and sequence alignment. *Brief Bioinform.* **5**, 150–163
23. Thompson, J.D., Higgins, D.G., and Gibson, T.J. (1994) CLUSTAL W: improving the sensitivity of progressive multiple sequence alignment through sequence weighting, position-specific gap penalties and weight matrix choice. *Nucleic Acids Res.* **22**, 4673–4680
24. Wayne, L.G. and Diaz, G.A. (1986) A double staining method for differentiating between two classes of mycobacterial catalase in polyacrylamide electrophoresis gel. *Anal. Biochem.* **157**, 89–92
25. Bertrand, T., Eady, N.A.J., Jones, J.N., Jesmin, Nagy, J.M., Jamart-Gregoire, B., Raven, E.L., and Brown, K.A. (2004) Crystal structure of *Mycobacterium tuberculosis* catalase–peroxidase. *J. Biol. Chem.* **279**, 38991–38999
26. Smulevich, G., Jakopitsch, C., Droghetti, E., and Obinger, C. (2006) Probing the structure and bifunctionality of catalase–peroxidase (KatG). *J. Inorg. Biochem.* **100**, 568–585
27. Pierattelli, R., Banci, L., Eady, N.A., Bodiguel, J., Jones, J.N., Moody, P.C., Raven, E.L., Jamart-Gregoire, B., and Brown, K.A. (2004) Enzyme-catalyzed mechanism of isoniazid activation in class I and class III peroxidases. *J. Biol. Chem.* **279**, 39000–39009
28. Fridovich, I. (1978) The biology of oxygen radicals. *Science* **201**, 875–880
29. Milano, A., Forti, F., Sala, C., Riccardi, G., and Ghisotti, D. (2001) Transcriptional regulation of *furA* and *katG* upon oxidative stress in *Mycobacterium smegmatis*. *J. Bacteriol.* **183**, 6801–6806
30. Hahn, J.S., Oh, S.Y., and Roe, J.H. (2000) Regulation of the *furA* and *catC* operon, encoding a ferric uptake regulator homologue and catalase–peroxidase, respectively, in *Streptomyces coelicolor* A3(2). *J. Bacteriol.* **182**, 3767–3774
31. Peterson, J.D., Umayam, L.A., Dickinson, T., Hickey, E.K., and White, O. (2001) The comprehensive microbial resource. *Nucleic Acids Res.* **29**, 123–125
32. Master, S., Zahrt, T.C., Song, J., and Deretic, V. (2001) Mapping of *Mycobacterium tuberculosis* katG promoters and their differential expression in infected macrophages. *J. Bacteriol.* **183**, 4033–4039
33. Pym, A.S., Domenech, P., Honoré, N., Song, J., Deretic, V., and Cole, S.T. (2001) Regulation of catalase–peroxidase (KatG) expression, isoniazid sensitivity and virulence by furA of *Mycobacterium tuberculosis*. *Mol. Microbiol.* **40**, 879–889
34. Zahrt, T.C., Song, J., Siple, J., and Deretic, V. (2001) Mycobacterial FurA is a negative regulator of catalase–peroxidase gene katG. *Mol. Microbiol.* **39**, 1174–1185
35. Sala, C., Forti, F., Di Florio, E., Canneva, F., Milano, A., Riccardi, G., and Ghisotti, D. (2003) *Mycobacterium tuberculosis* FurA autoregulates its own expression. *J. Bacteriol.* **185**, 5357–5362
36. Sala, C., Forti, F., Magnoni, F., and Ghisotti, D. (2008) The katG mRNA of *Mycobacterium tuberculosis* and *Mycobacterium smegmatis* is processed at its 5′ end and is stabilized by both a polypurine sequence and translation initiation. *BMC Mol. Biol.* **9**, 33
37. Wariishi, H., Valli, K., and Gold, M.H. (1992) Manganese(II) oxidation by manganese peroxidase from the basidiomycete *Phanerochaete chrysosporium*. Kinetic mechanism and role of chelators. *J. Biol. Chem.* **267**, 23688–23695
38. Magliozzo, R.S. and Marcinkeviciene, J.A. (1997) The role of Mn(II)-peroxidase activity of mycobacterial catalase–peroxidase in activation of the antibiotic isoniazid. *J. Biol. Chem.* **272**, 8867–8870
39. Kono, Y. and Fridovich, I. (1983) Isolation and characterization of the pseudocatalase of *Lactobacillus plantarum*. *J. Biol. Chem.* **258**, 6015–6019
40. Allgood, G.S. and Perry, J.J. (1986) Characterization of a manganese-containing catalase from the obligate thermophile *Thermoleophilum album*. *J. Bacteriol.* **168**, 563–567
41. Ivancich, A., Barynin, V.V., and Zimmermann, J.L. (1995) Pulsed EPR studies of the binuclear Mn(III) Mn(IV) center in catalase from *Thermus thermophilus*. *Biochemistry* **34**, 6628–6639
42. Zou, P. and Schrempf, H. (2000) The heme-independent manganese-peroxidase activity depends on the presence of the C-terminal domain within the *Streptomyces reticuli* catalase–peroxidase CpeB. *Eur. J. Biochem.* **267**, 2840–2849
43. Glenn, J.K. and Gold, M.H. (1985) Purification and characterization of an extracellular Mn(II)-dependent peroxidase from the lignin-degrading basidiomycete, *Phanerochaete chrysosporium*. *Arch. Biochem. Biophys.* **242**, 329–341
44. Glenn, J.K., Akileswaran, L., and Gold, M.H. (1986) Mn(II) oxidation is the principal function of the extracellular Mn-peroxidase from *Phanerochaete chrysosporium*. *Arch. Biochem. Biophys.* **251**, 688–696
45. Sundaramoorthy, M., Kishi, K., Gold, M.H., and Poulos, T.L. (1994) The crystal structure of manganese peroxidase from *Phanerochaete chrysosporium* at 2.06-A resolution. *J. Biol. Chem.* **269**, 32759–32767
46. Goldberg, I. and Hochman, A. (1989) Purification and characterization of a novel type of catalase from the bacterium *Klebsiella pneumoniae*. *Biochim. Biophys. Acta.* **991**, 330–336
47. Love, D.N. and Redwin, J. (1994) Characterization of the catalase of the genus *Porphyromonas* isolated from cats. *J. Appl. Bacteriol.* **77**, 421–425
48. Calera, J.A., Sánchez-Weatherby, J., López-Medrano, R., and Leal, F. (2000) Distinctive properties of the catalase B of *Aspergillus nidulans*. *FEBS Lett.* **475**, 117–120
49. Kang, Y.S., Lee, D.H., Yoon, B.J., and Oh, D.C. (2006) Purification and characterization of a catalase from photosynthetic bacterium *Rhodospirillum rubrum* S1 grown under anaerobic conditions. *J. Microbiol.* **44**, 185–191
50. Carpena, X., Loprasert, S., Mongkolsuk, S., Switala, J., Loewen, P.C., and Fita, I. (2003) Catalase–peroxidase KatG of *Burkholderia pseudomallei* at 1.7A resolution. *J. Mol. Biol.* **327**, 475–489

51. Marttila, H.J., Soini, H., Eerola, E., Vyshnevskaya, E., Vyshnevskiy, B.I., Otten, T.F., Vasilyef, A.V., and Viljanen, M.K. (1998) A Ser315Thr substitution in KatG is predominant in genetically heterogeneous multidrug-resistant *Mycobacterium tuberculosis* isolates originating from the St. Petersburg area in Russia. *Antimicrob. Agents Chemother*. **42**, 2443–2445
52. Ramaswamy, S. and Musser, J.M. (1998) Molecular genetic basis of antimicrobial agent resistance in *Mycobacterium tuberculosis*: 1998 update. *Tuber. Lung Dis*. **79**, 3–29